JETIR.ORG ISSN: 2349-5162 | ESTD Year : 2014 | Monthly Issue
JOURNAL OF EMERGING TECHNOLOGIES AND INNOVATIVE RESEARCH (JETIR)
An International Scholarly Open Access, Peer-reviewed, Refereed Journal

Explainable Lightweight Vision Transformer with Recurrent Neural Network for Brain Hemorrhage Detection and Classification using Biomedical Images

[1]S. Sandhya, [2]Dr. R. Karunia Krishnapriya, [3]T. Senthil

[1]PG Scholar, [2,3]Associate Professor

[1, 2, 3]Department of Computer Science and Engineering, Sreenivasa Institute of Technology and Management studies, Chittoor.

Abstract : Intracranial hemorrhage (ICH) is a serious potential neurological condition. Among the normal causes of ICH is traumatic brain injury. Computed Tomography (CT) scans are generally employed in the crucial assessment of patients to diagnose ICH and capture several layers of the brain. Nonetheless, this procedure could be lengthy, and subspecialty-trained neuroradiologists are not always accessible for evaluation. Artificial intelligence (AI), especially deep learning (DL) models and convolutional neural network (CNN) has shown exceptional outcomes for automating the segmentation and detection of ICH areas from CT imaging. These AI models could considerably decrease diagnosis time and improve healthcare process efficacy, particularly in emergencies. Although a main problem in deploying these useful AI techniques in crucial medical settings is their black box nature. Hence, explainable artificial intelligence (XAI) models are incorporated that offer interpretable and transparent insights. This manuscript presents a Hybrid Deep Learning-Based Framework for Intracranial Hemorrhage Detection (HDLF-ICHD). This study aims to develop an intelligent system capable of effectively identifying and classifying intracranial hemorrhage from medical images while providing visual interpretability of the model decisions. Towards that aim, the proposed HDLF-ICHD model initially preprocesses input images using a wiener filter for noise removal and CLAHE for contrast enhancement. Subsequently, TransUNet optimized with RMSProp is utilized for precise hemorrhage segmentation. Discriminative features are then extracted using a lightweight vision transformer architecture. The extracted features are fed into a convolutional multi-head attention recurrent neural network for classification, with RMSProp utilized for hyperparameter optimization. To improve medical interpretability, Grad-CAM++ is integrated to visualize salient regions influencing the model's decision-making. A series of experimental analyses is made, and the results are inspected under multiple performance measures. The comparison study showed the improved performance of the HDLF-ICHD technique compared to existing approaches.

IndexTerms **- Intracranial Hemorrhage; Medical Image Analysis; Transunet; Deep Learning; Feature Extraction; Attention-Based Classification; Explainable Artificial Intelligence.**

I. INTRODUCTION

An intracranial hemorrhage (ICH) comprises bleeding that arises in the cerebrospinal fluid. This disease illustrates a hazardous health issue that needs early analysis and treatment [1]. ICHs account for nearly 10 to 30% of strokes, but that is the most hazardous category of stroke, accounting for 35 to 52% of demises in comparison with other strokes [2]. The most significant factors of an ICH are weak blood vessels, high blood pressure, and the skull's exterior trauma, drug use, and the entry of blood into the bloodstream, correlated to the ICH. The main categories of ICHs are subdural, subarachnoid, epidural, intraparenchymal, and intraventricular hemorrhages. So, early detection and treatment of the case is required, since such cases could be fatal for the patients if they are infected [3]. For clinical therapy of grievances that occur due to brain hemorrhaging, identifying the category and finding the bleeding position is necessary for the treatment. Consequently, computed tomography (CT), the referred evaluation for medical diagnosis of ICHs, is appropriate, fast, and includes a clear effect [4]. CT is considered the finest medical approach utilized to analyse the cause of brain hemorrhages, its merits, like its higher compassion to blood, and the scanning time is lesser, exposing the hemorrhagic region with higher density [5]. Moreover, this approach is difficult and time-consuming, posing challenges to apply in medical practice.

The field of Artificial Intelligence (AI) has shown an important role in the clinical imaging field. Between each other, only a few analyses have been made to identify abnormalities in skull CT and ICH using Machine Learning (ML) models [6]. Deep Learning (DL) models belong to the subset of ML that includes the capability to automate the diagnosis process for the recognition of cerebral hemorrhage. These systems automatically execute feature recognition and classification, therefore mitigating the manually derived feature hand-made step conducted as one of the ML algorithms [7]. Especially, convolutional neural networks (CNNs) are established that the model has a great performance in automating various image classification and partition operations [8]. In addition, some researches need to concentrate on comparing various pre-trained deep CNN architectures that enable fine-tuning

and adaptation, and a few others focus on designing a deep NN developed from the basics for the ICH classification operation [9]. It can be monitored that shows a dearth of analysis that employs the selection of feature technique coupled with the DL model for classification tasks [10]. The presentation of a feature selection part can assist in choosing the most distinctive features for the enhanced classification process of the DL framework.

This paper proposes a Hybrid Deep Learning-Based Framework for Intracranial Hemorrhage Detection (HDLF-ICHD) for detecting and classifying ICH from medical images while ensuring visual interpretability of the model decisions. The proposed model integrates comprehensive steps: First, the Wiener filter (WF) and CLAHE are applied to enhance the input image quality for further analysis. Afterwards, used a TransUNet optimized with RMSProp for accurate hemorrhage segmentation. The crucial features are then extracted through a lightweight vision transformer (LeViT) model. The extracted high-level features are input to a convolutional multi-head attention recurrent neural network (CMHA-RNN), which is the combination of CNN, multi-head attention (MHA), and bi-directional long short-term memory (BiLSTM) for classification, with RMSProp deployed to fine-tune model parameters. For clinical interpretability, this study integrates Grad-CAM++ for visualizing salient regions influencing the model's decision-making process. Finally, an experimentation analysis is carried out, and the outcomes are evaluated. The comparison study indicated the superiority of the HDLF-ICHD model compared to recent models.

II. Related Studies

This section offers a concise review of the relevant literature on ICH detection and classification using CT images. Yenkikar et al. [11] presented a DL approach for detecting severe ICH, categorizing it into its subclasses, and the major challenge we intended to achieve was to segment the site of hemorrhage. DL-based methods in medical imaging could be implemented on the CT images for ICH segmentation and detection more effectively than other techniques. The author also intended to use this system as a cloud service. AI on the cloud creates an intellectual system available to all without the need for progressive skills, and makes it easier to expand as projects go into production. Lin et al. [12] introduced an innovative Attention-Based Residual U-Net (ResUNet) technique for precisely dividing various kinds of brain hemorrhages from CT scans. This method intends to address the restrictions of current automated and manual segmentation algorithms concerning generalizability and precision. Furthermore, complete CT images were consistent with a standard anatomic space, and strength normalization has been implemented for consistency. The ResUNet method contains attention mechanisms for enhancing the concentration on residual connections and significant features for supporting the efficient gradient and stable learning flow. Hassan et al. [13] presented a DL approach intended to enable an efficient and precise classification of ICH in CT scan images. The above-mentioned method concentrates on improving U-Net-based algorithms for the segment of ICH. Also, this technique is used in two transfer learning (TL) systems, Xception and MobileNet, which are the main support for the U-Net topology. The above technique is intended for establishing the metrics that develop the ICH treatment with accurate segmentation approaches.

Rajapakse et al. [14] presented a two-phase method that employs both segmentation masks and bounding boxes for improvements in the segmentation process. In the initial phase, ICH areas are localized and identified through bounding boxes near the lesion by utilizing a supervised YOLOv5 object sensor. Though the author uses both segmentation masks and ground-truth bounding boxes, various datasets could be utilized for training and staging. Ahmed et al. [15] introduced a DL and standard ML techniques, with the intention of dependably and promptly classifying and identifying brain hemorrhage. The above research gives a complete examination of the surveys that have been conducted using ML and DL techniques. This study concentrates on the key phases of brain haemorrhage that contain feature extraction, classification, and pre-processing, as well as their limitations and findings. Gençtürk et al. [16] proposed a processing of computed tomography (CT) images through DL algorithms and their part in the analysis of brain hemorrhages, a DL-based model for precisely segmenting and detecting brain hemorrhages. The above-mentioned system integrates the frameworks of EfficientNet-B2 and Mask Scoring R-CNN, providing an effective technique for the classification and recognition of brain hemorrhages. Therefore, this approach provides a two-phase verification procedure that improves accuracy and precision.

III. Proposed Framework

The proposed HDLF-ICHD model consists of a structured DL pipeline developed for precise ICH detection and classification. Fig. 1 illustrates the workflow of the proposed HDLF-ICHD model. As exhibited in Fig. 1, this study begins with an image preprocessing stage, where a WF is applied to reduce noise, followed by CLAHE to improve image contrast and enrich the visibility of hemorrhagic regions. After preprocessing, hemorrhage localization is carried out using TransUNet optimized with RMSProp, which allows for accurate segmentation of affected areas. Once segmentation is done, discriminative feature representations are obtained using a LeViT model, which efficiently extracts local as well as global contextual information. The extracted features are further provided to a CMHA-RNN for hemorrhage classification, which is also optimized using RMSProp to enhance learning stability and convergence. Lastly, Grad-CAM is utilized to generate visual explanations that emphasize the salient regions contributing to the model's predictions, resulting in enhanced clinical interpretability.

3.1 Image Preprocessing

In the proposed model, the input CT images are initially preprocessed to enhance image quality and improve diagnostically relevant features.

Noise Removal: The WF is a commonly employed filter in the field of frequency [17]. Blurred images are restored by Inverse Filtering (IF), but it is extremely sensitive to additive noise, frequently expanding it during deblurring. The WF lessens the Mean Squared Error (MSE) to balance image restoration and noise reduction, offering a linear and stronger approximation of original image. IF could restore images blurred by low-pass filters, but it is extremely sensitive to additive noise, increasing both noise and blur.

$$W(f_{1t}f_2) = \frac{H^*(f_{1'}f_2)S_{\chi\chi}(f_{1'}f_2)}{|H(f_{1'}f_2)|^2 S_{\chi\chi}(f_1f_2) + S_{nn}(f_{1'}f_2)} \quad (1)$$

Now, $H(f_{1,}f_2)$ denotes the filter's frequency transfer function; $s_{nn}(f_{1t}f_2)_t$ and $s_{\chi\chi}(f_{1t}f_2)$ implies the power spectra of additional noise and original image, correspondingly.

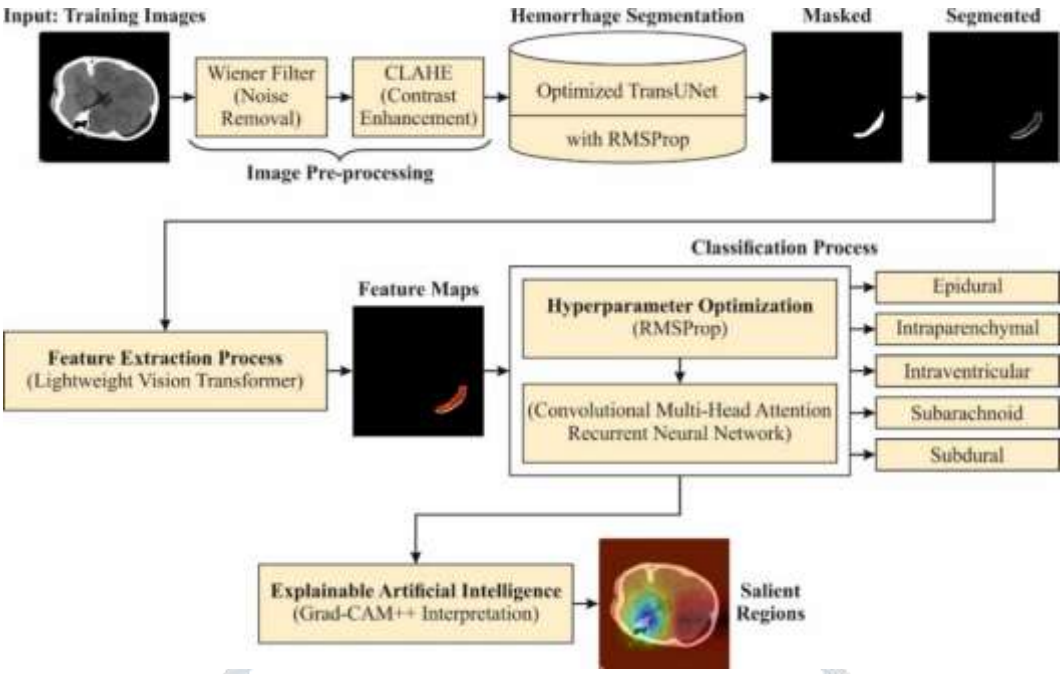

Fig. 1. Workflow of the proposed HDLF-ICHD model

CLAHE: CLAHE is a sophisticated image enhancement model which enhances local contrast to redistribute value of intensity in diverse regions [18]. The traditional histogram equalization employs global transformation, CLAHE separates the image into smaller non-overlapping tiles, and every tile undergoes autonomous equalization of histogram. Here, the image has been separated into smaller tiles, and every tiles are required to separate histogram equalization procedure. The upgraded image has been attained to employ the cumulative distribution function of histogram, the input image I with values ranging among $[0, L]$. The clip function is clipping to range 0 and L, and is set 2 refining contrast enhancement and avoid noise.

$$CLAHE\left(I_{(h,w)}\right) = clip\left(\frac{CDF(I) - CDF_{\min}}{CDF_{\max} - CDF_{\min}} \times L\right) \quad (2)$$

3.2 Hemorrhage Segmentation Using TransUNet

For the precise localization of hemorrhagic regions, TransUNet optimized with the RMSProp optimizer is utilized to perform precise segmentation. In segmentation, an instinctive outcome is easily upsample the encoded depiction of feature $z_L \in R^{\frac{HW}{P^2} \times D}$ to entire resolution to predict the dense outcomes [19]. To restore the spatial sequence, the dimensions of encoded aspects are reshaped from $\frac{HW}{P^2}$ to $\frac{H}{P} \times \frac{W}{P}$. To employ a 1x1 convolution by decreasing channel size of reshaped aspects to class counts, and then mapping feature was bilinearly upsampled to full resolution HxW to predict the outcome of final segmentation. While integrating a transformer with naive upsampling that generates beneficial outcomes, this approach is not the optimum utilization of transformers in segmentation, meanwhile $\frac{H}{P} \times \frac{W}{P}$ is typically lower than the novel image resolution HxW, thus certainly induces a loss of lower-level particulars.

CNN-Transformer Hybrid Encoder: Instead of utilizing the original transformer as encoder, TransUNet leverages a CNN-Transformer hybrid technique. Here, CNN was utilized as a feature representation model by generating a mapping feature for input. Patch embedding has been employed to 1x1 patches acquired from CNN mapping features rather than raw images. To select this model, primarily it enable for employing the in-between CNN feature mapped in decoder path; and then discover the hybrid CNN-Transformer encoded achieves improved than easily utilizing a pure transformer as encoder.

Cascaded Upsampler: To present a CUP that comprises numerous upsampling stages by decoding the hidden aspects for outputs the ending task of segmentation. Once reshape the order of hidden aspect $z_L \in R^{\frac{HW}{P^2} \times D}$ to the shape of $\frac{H}{P} \times \frac{W}{P} \times$ D, to instantiate CUP to cascade numerous upsampling blocks to reach the full resolution from $\frac{H}{P} \times \frac{W}{P}$ to H×W, here every block comprises 2×2 upsampling operator, 3×3 convolution layer, and ReLU layer consecutively.

Root Mean Square Propagation (RMSprop) is a rate of adaptive learning that modifies the dimension of step by averaging the squared gradient of every parameter [20]. This module aids to balance rate of learning in training. RMSprop has effectual to enhance non-stationary objective functions, those experienced in training RNNs. The succeeding calculations depict the key stages in the RMSprop model: gradient assessment, running average of squared gradients, and parameter updates with the rate of learning actively modified depending on the accumulated data from gradient history.

$$g_t = \nabla_{\theta_t L}(\theta_r) \quad (3)$$

$$v_t = v_{t-1} + (1 - \beta) g_t^2 \quad (4)$$

$$\theta_{t+1} = \theta_t - \frac{\alpha}{\sqrt{v_t + \varepsilon}} g_t \quad (5)$$

Here, v_t denotes exponentially weight average of square gradients; g_t signifies the existing gradient; β implies decay factor; α refers to the rate of learning, and ϵ depicts smaller constant to impede division by 0.

3.3 Feature Extraction Module

Following segmentation, discriminative features are captured using a LeViT architecture to represent hemorrhage patterns efficiently. Hybrid DL techniques, LeViT, that integrate the advantages of CNN and ViT towards categorizing the relevant classes [21]. It is intended for regulating both local aspects together with global dependency in images. The framework starts with the backbone of CNN that acquires hierarchical aspects from input image. It accomplished by a sequence of convolution layers, every layer employs a group of learnable filters K succeeded by an activation function of ReLU.

$$F_{CNN} = f_{CNN} = \Sigma_{i=1}^{C_{in}} \Sigma_{j=1}^{k \times k} W_{i,j} * I_{i,j} + b \rightarrow Conv2D(K, ReLU) \quad (6)$$

The backbone of CNN assures that local special aspects are effectively acquired by examining comprehensive steps as components in differences. Furthermore, the mapping feature F_{CNN} was separated into non-overlapping patches, which are compressed and estimated into lower dimension space utilizing a learnable projection matrix W_p. This process is named batch embedding.

$$z_o = \left[x_p^1 W_{P'} x_p^2 W_{P''} \dots \dots x_p^N W_p\right] + E_{pos} \quad (7)$$

Additionally, Encoder Transformer comprises numerous layers of MSA and FFNs. Self-attention module evaluates attention scores through every patch embedding so as to longer-range dependency can also learnt by techniques.

$$z, = Layer\_Norm(z_1 + Concate\left(Atten\left(z_1 W_Q^i, z_1 W_K^i, z_1 W_V^i\right)\right)_{i=1}^h W_O) \quad (8)$$

Eventually, the categorization head processes the outcome feature vector z_1 by FC layer with SoftMax activation by generating class likelihoods.

$$P(y|I) = soft\max\left(W^T z_L + b\right) \quad (9)$$

The function of SoftMax generates the outcome probability distribution across classes.

3.4 Attention-Based Classification Approach

The extracted feature representations are then processed by a CMHA-RNN to perform accurate hemorrhage classification, with RMSProp utilized for hyperparameter tuning. This method is an effective mechanism utilized in the domain of ML, especially in series modeling [22]. It covers the idea of attention mechanism (AM) by enabling the method to jointly attend to data from various depictions sub-spaces at various locations. It is attained throughout many attention heads, all concentrating on several features of the order of input. Officially, provided an input order, the MHA module executes the succeeding stages:

- Linear Projections: The order of input has linear approximation into several subspaces employing various groups of learned projection matrices. The projection process various groups of key (K), value (V), and query (Q).
- Scaled Dot-Product Attention: For all groups of estimations, the scaled dot-product attention has been calculated.
- Concatenation: The outcomes of each attention head are concatenated to form a unique vector.
- Final Linear Projection: This concatenated outcome is the linear projection to process the last attention outcomes.

$$Multi_{Head}(Q, K, V) = Concate(head_1, head_2, \dots, head_h) W^O \quad (10)$$

Here, every head i is calculated as:

$$head_i = Atten\left(QW_i^Q, KW_i^K, VW_i^V\right) \quad (11)$$

Let W_i^Q, W_i^K, W_i^y, and W^O denotes the learned projection matrices.

The major benefits of MHA are that it enables the method for capturing various kinds of relations and dependency inside the information to attend to the several parts of the sequence of input concurrently. The mechanism improves the method's capability of understanding intricate patterns and interactions, making it especially efficient for challenges, including contextual and sequential information.

Convolutional BiLSTM

This network is a hybrid method that integrates convolution with Bi-LSTM layers for leveraging both spatial-temporal dependency in consecutive information. This structure is especially efficient for challenging situations whereas both local feature extractor and longer-range dependency are critical.

Convolutional Layers

This layer is intended for local feature extraction from input information. Where X denotes the sequence of input, here X implies the size matrix $T \times D$, where T represents the order of length, and D denotes the dimension of all input vectors. A $1D$ convolution function is used for X, utilizing a filter W to process a feature mapped F:

$$F_i = ReLU\left(\sum_{j=1}^{k} W_j \cdot X_{i+j-1} + b\right) \quad (12)$$

Let k imply the size of the filter, b imply the term of bias, and ReLU signifies the activation function of Rectified Linear Unit.

Bidirectional LSTM

This layer element improves the technique by integrating both future and past contexts into the learning procedure. For all time steps z, the LSTM of forward calculates hidden states $\overrightarrow{h_z}$ and the LSTM of backward calculates hidden states $\overleftarrow{h_z}$.

$$\overrightarrow{f_z} = \sigma\left(W_f \cdot \left[\overrightarrow{h_{z-1}}, x_z\right] + b_f\right) \quad (13)$$

$$\overrightarrow{i_{t=z}} = \sigma\left(W_i \cdot \left[\overrightarrow{h_{z-1}}, x_z\right] + b_i\right) \quad (14)$$

$$\overrightarrow{c_z} = \overrightarrow{f_z} \cdot \overrightarrow{c_{z-1}} + \overrightarrow{i_z} \cdot \tanh\left(W_c \cdot \left[\overrightarrow{h_{z-1}} x_z\right], + b_c\right) \quad (15)$$

$$\overrightarrow{o_z} = \sigma\left(W_o \cdot \left[\overrightarrow{h_{z-1}}, x_z\right] + b_o\right) \quad (16)$$

$$\overrightarrow{h_z} = \overrightarrow{o_z} \cdot \tanh\left(\overrightarrow{c_z}\right) \quad (17)$$

Here, σ signifies the function of sigmoid, and W_f refers the weighted matrices of forgetting gate, W_i implies the weighted matrices of inputting gate, W_c represents weighted matrices of cell gate, and W_o implies weight matrices for the output gate, correspondingly. The LSTM of backward calculates same upgrades but in the reverse direction.

The last hidden state h_t at every time step is to concatenate the forward as well as backward hidden states:

$$h_t = [\overrightarrow{h_t}, \overleftarrow{h_t}], \tag{18}$$

Here,] implies concatenation.

Integrating Convolution and Bi-LSTM Layers

In this approach, the outcomes of the convolution layers that acquire local characteristics are supported into the layer of BiLSTM. This integration enables the technique for significant local features extraction and also takes temporal dependency in both directions, improving its capability of understanding intricate models in the information. The Convolution BiLSTM structure combines convolution layers with BiLSTM to solve both temporal and local features of consecutive information. The convolution layers serve as feature extraction, which captures spatial dependency inside local areas of the order of input, offering a group of feature maps that signify various features of the information. This feature mapping is then processed by the bidirectional LSTM layers that utilize Bi-LSTM for capturing longer-range dependency to consider both future and past contexts. The BiLSTM enables the technique for learning from data that is received from both directions in order, thus enhancing the comprehension of intricate patterns and relations. This hybrid method improves the method's capability for handling sequential information with complex temporal dynamics and spatial framework, creating it suitable for challenges like tornado forecasts where both global and local characteristics are crucial for precise outcomes. The classification module is further optimized using the RMSProp optimizer for improved model generalization and classification performance.

Model interpretability using Grad-CAM++

To improve transparency and clinical trust, Grad-CAM++ is integrated for generating visual explanations highlighting regions that influence the model's predictions. The Grad-CAM++ model aims to improve interpretability and transparency of DL technique [23]. Grad-CAM++ is a post hoc XAI method that makes finer and more comprehensive heat mapping to utilize high-order gradient data, making it especially efficient for intricate healthcare imaging.

A class-specific significance weight α_{ij}^{kc} has been made for every spatial position (i, j) in every feature mapping channel k. In Grad-CAM++, this is attained to integrates 2nd and 3rd-order partial derivatives of outcomes y^c concerning the spatial characteristics A_{ij}^k, calculated as

$$\alpha_{ij}^{kc} = \frac{\frac{\partial^2 y^c}{(\partial A_{ij}^k)^2}}{2\frac{\partial^2 y^c}{(\partial A_{ij}^k)^2} + \Sigma_{a,b} A_{ab}^k \frac{\partial^3 y^c}{(\partial A_{ij}^k)^3}} \tag{19}$$

Here, A_{ij}^k implies the value of activation at position (i, j) in k_{th} feature mapping, and the derivatives signify compassion of class score to activations. Afterward, the class activation mapping $L_{Grad-CAM++}^c$ has been created to aggregate the calculated weights α_{ij}^{kc} and positive gradients:

$$L_{Grad-CAM++}^c = \sum_k \sum_i \sum_j \alpha_{ij}^{kc} . ReLU\left(\frac{\partial y^c}{\partial A_{ij}^k}\right) \tag{20}$$

When $L_{Grad-CAM++}^c$ is calculated, bilinear interpolation is used for resizing the heatmap by comparing the size of the real input imaging. The last outcome is a color-coded overlay on the input image, where brighter areas highlight robust impact on the method's forecast. Some visual explanations were critical to assist clinical specialist in verifying but the model's decision relies on clinically significant characteristics.

IV. Findings and Interpretation

In this section, the performance analysis of the HDLF-ICHD system is inspected under the intracranial hemorrhage dataset [24]. Computed Tomography (CT) images are broadly used for segmenting and identifying intracranial hemorrhage because of their availability, speed, and higher sensitivity to acute bleeding. Such images clearly differentiate hemorrhagic regions as hyperdense areas related to normal brain tissue. Automated segmentation and detection methods analyze CT scans to precisely localize hemorrhage size, shape, and type. This helps clinicians in rapid analysis and treatment planning. These techniques reduce interpretation time, increase accuracy, and assist emergency decision-making. Fig. 2 depicts the sample images of original, pre-processed, masked, segmented, and feature maps.

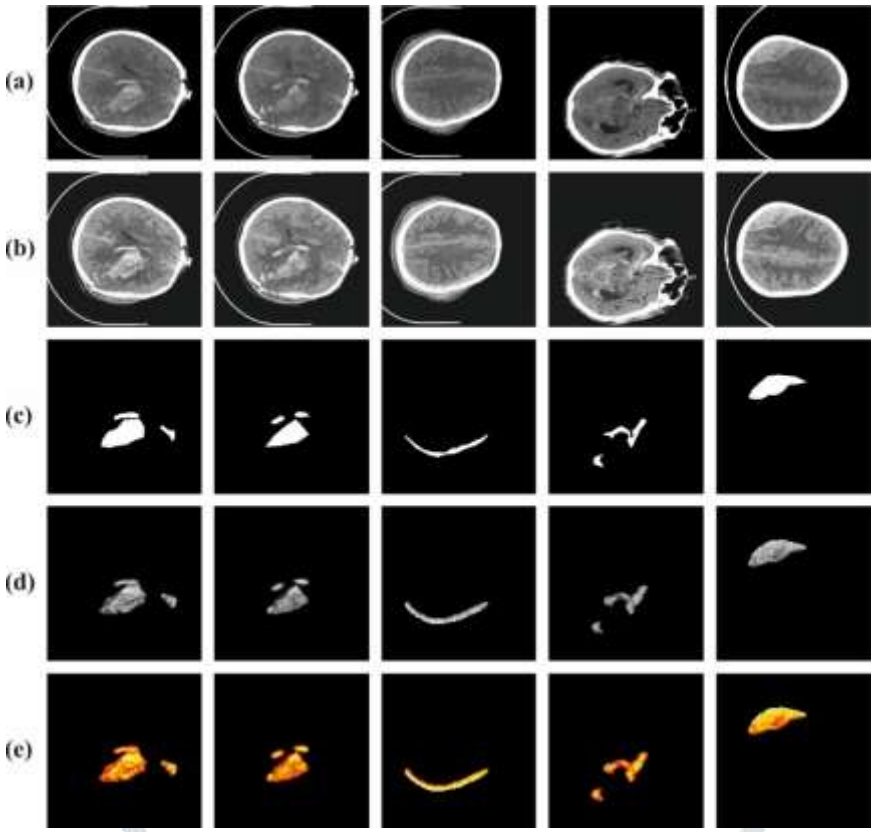

Fig. 2. Sample images of (a) original, (b) pre-processed, (c) masked, (d) segmented, (e) feature maps

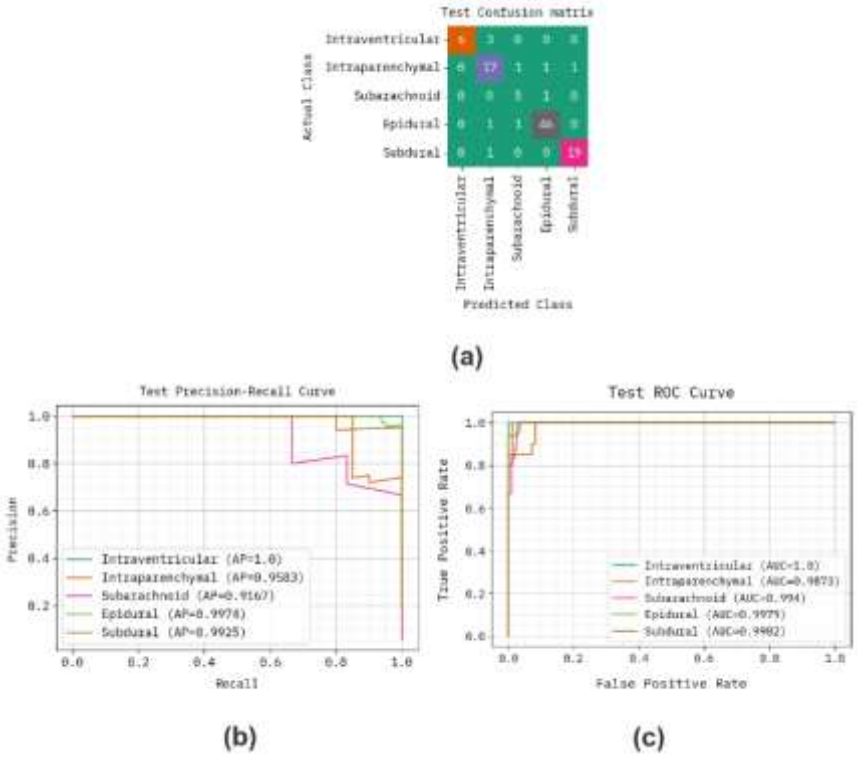

Fig. 3. HDLF-ICHD method (a) confusion matrix, (b) PR, and (c) ROC curves

Fig. 3 depicts the classifier results of the HDLF-ICHD approach from TRAP and TESP. Fig. 3a displays the confusion matrix with precise classification and detection of 5 class labels. Fig. 3b represents the PR analysis, representing maximum performance over 5 classes. Finally, Fig. 3c establishes the ROC examination, signifying proficient result with great ROC for different class label.
Fig. 4 establishes the classifier outcomes of the HDLF-ICHD system. Fig. 4a determines the precision analysis of the HDLF-ICHD technique. The figure indicates that the HDLF-ICHD model attains improved values across increasing epochs. Also, the growing validation across training displays that the HDLF-ICHD approach learns efficiently on the dataset. Later, Fig. 4b shows the loss analysis of the HDLF-ICHD approach. The outcomes suggest that the HDLF-ICHD system gains closer outcomes of training and validation loss. It is observed that the HDLF-ICHD model learns proficiently on the dataset. Furthermore, Fig. 4c illustrates the dice loss for testing and training, where a sharp reduction in initial epochs followed by gradual stabilization shows better overlap among predicted and ground-truth segmentation masks. Lastly, Fig. 4d establishes that the IOU metric of the HDLF-ICHD method

is revealed. The outcomes recommended that the HDLF-ICHD approach achieves IoU values with a rise in epochs. Consequently, the HDLF-ICHD system reaches decreasing loss values across improved epochs.

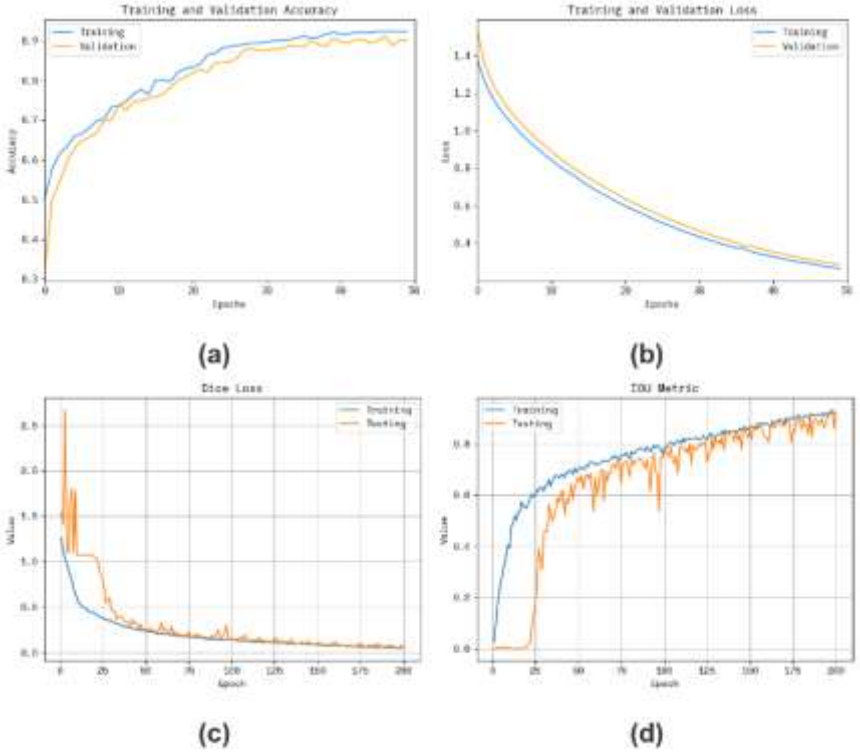

Fig. 4. HDLF-ICHD method (a, b) $accur_y$ and loss curves, (c, d) dice loss and IOU metric

The comparative analysis of the HDLF-ICHD method with other current models is given in Table 1 and Fig. 5 [25, 26]. The investigational results inferred that the HDLF-ICHD system has shown improved performance. Depend on $accur_y$, the proposed HDLF-ICHD approach gains maximal performance with $accur_y$ of 93.28%, whereas the ResNexT, SVM, CNN, U-Net, WA-ANN, Joint CNN-RNN, and DGPMIL systems obtained minimal results with $accur_y$ of 90.71%, 78.24%, 87.63%, 87.50%, 70.27%, 88.00%, and 82.50%, respectively. In addition, depend on $preci_n$, the proposed HDLF-ICHD algorithm gains a greater result with $preci_n$ of 86.00% while the ResNexT, SVM, CNN, U-Net, WA-ANN, Joint CNN-RNN, and DGPMIL models had lesser results with $preci_n$ of 84.86%, 79.27%, 81.98%, 80.39%, 71.94%, 78.95%, and 82.59%, correspondingly. Finally, depending on MCC, the proposed HDLF-ICHD approach achieves higher performance with MCC of 83.87%, whereas the ResNexT, SVM, CNN, U-Net, WA-ANN, Joint CNN-RNN, and DGPMIL methodologies attained lower outcomes with MCC of 76.22%, 81.09%, 82.32%, 75.28%, 74.94%, 80.63%, and 82.06%, respectively.

Table 1. Comparative Outcomes HDLF-ICHD Method with Existing Models

Algorithms	$Accur_y$	$Preci_n$	$Sens_y$	$Spec_y$	$F1_{Score}$	MCC
ResNexT	90.71	84.86	80.84	90.78	80.90	76.22
SVM	78.24	79.27	75.12	78.64	81.18	81.09
CNN	87.63	81.98	83.61	88.94	75.09	82.32
U-Net	87.50	80.39	64.54	87.21	83.14	75.28
WA-ANN	70.27	71.94	64.87	72.15	84.02	74.94
Joint CNN-RNN	88.00	78.95	84.36	81.17	79.70	80.63
DGPMIL	82.50	82.59	82.03	84.56	75.90	82.06
HDLF-ICHD	93.28	86.00	85.09	98.28	85.44	83.87

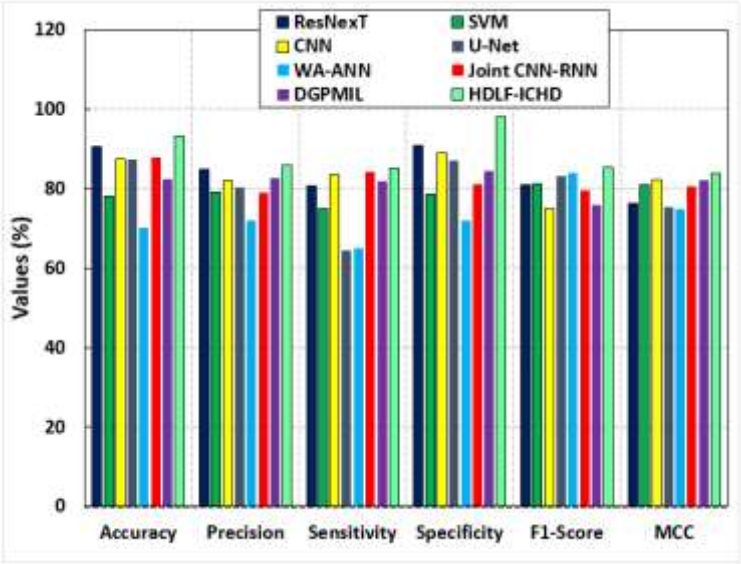

Fig. 5. Comparative outcomes of HDLF-ICHD method with existing techniques

Fig. 6 shows the visual interpretation of the GradCAM++ with other XAI approaches. The figure suggests that various CAM++ methods are implemented for providing visual interpretation for abnormality identification. Such techniques give a heatmap representing the regions on the input image important for making decisions by the implemented systems. The figure displays CT brain images overlaid with XAI heatmaps, like Grad-CAM++, employed for intracranial hemorrhage examination. The colored regions suggest areas where the DL technique concentrates on most intensely while making its predictions. Higher-intensity colors (red/yellow) highlight medically appropriate hemorrhagic regions, while lower-activation regions (blue/green) suggest less importance. This visualization shows that the algorithm learns meaningful, pathology-specific features instead of background noise. Generally, these explanations increase model trustworthiness, transparency, and clinical intelligibility in medical imaging applications.

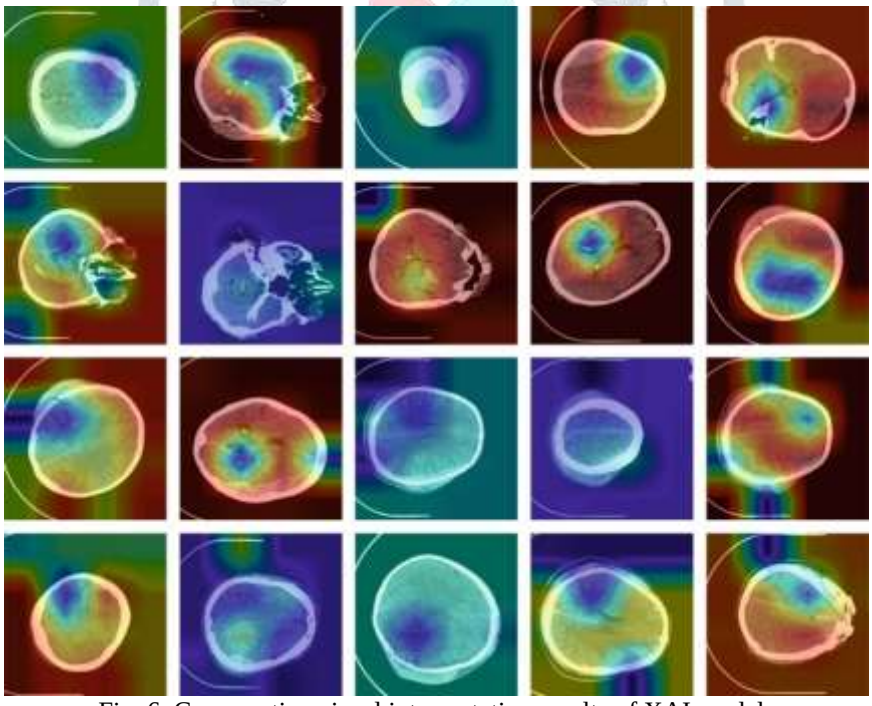

Fig. 6. Comparative visual interpretation results of XAI models

V. Conclusion

This paper has proposed the HDLF-ICHD model to identify and classify ICH from CT scans while ensuring visual interpretability of the model decisions. To achieve this, the proposed HDLF-ICHD method primarily preprocesses input images with a WF to remove noise and CLAHE for enhanced contrast. Then, TransUNet optimized with RMSProp is employed for accurate hemorrhage segmentation. Afterwards, high-level discriminative features are captured using a LeViT model. The extracted features are passed into a CMHA-RNN architecture for classification, with RMSProp leveraged for hyperparameter optimization. To improve clinical interpretability, Grad-CAM++ is incorporated to visualize salient areas that contribute most to the decision-making process of the model. An extensive study is conducted, and the results are examined under diverse measures. The comparison study demonstrated the better performance of the HDLF-ICHD model compared to existing models

REFERENCES

[1] Mandhare, R.M. and Kshirsagar, D.B., 2026. Elk Herd Taylor Optimizer-based Deep Kronecker Network for stroke detection using brain computed tomography images. *Biomedical Signal Processing and Control*, *112*, p.108450.

[2] Ahmed, S.N. and Prakasam, P., 2025. Intracranial hemorrhage segmentation and classification framework in computer tomography images using deep learning techniques. *Scientific Reports*, *15*(1), p.17151.

[3] Sindhura, C. and Gorthi, S., 2025. A clinically knowledgeable, synthesized CT image-based framework for improved detection and segmentation of hemorrhages. *Pattern Recognition Letters*, *188*, pp.46-52.

[4] Dash, P., Sabut, S.K., Mishra, R., and Mishra, B.S.P., 2025, February. A hybrid CNN-LSTM approach for detecting intracerebral hemorrhage in CT images. In *2025 International Conference on Computer, Electrical & Communication Engineering (ICCECE)* (pp. 1-5). IEEE.

[5] Iesmantas, T., Petkus, V., Alzbutas, R., Barkauskiene, A., Ratkūnas, V., Lukosevicius, S., Preiksaitis, A., Lapinskiene, I., Serpytis, M., Misiulis, E. and Skarbalius, G., 2025. Semantic Segmentation and Quantification of Subarachnoid Hemorrhage of Cerebral CT Using Deep Convolutional Neural Networks. *International Journal of Imaging Systems and Technology*, *35*(3), p.e70104.

[6] Ramananda, S.H. and Sundaresan, V., 2025. Label-efficient sequential model-based weakly supervised intracranial hemorrhage segmentation in low-data non-contrast CT imaging. *Medical Physics*, *52*(4), pp.2123-2144.

[7] Xu, W., Sha, Z., Tan, T., Liu, W., Chen, Y., Li, Z., Pan, X., Jiang, R., and Yang, H., 2024. Automatic segmentation of intracranial hemorrhage in computed tomography scans with convolutional neural networks. *Journal of Medical and Biological Engineering*, *44*(4), pp.575-581.

[8] Babu, P.P.S. and Brindha, T., 2024, August. CT Scans Reimagined: Early Intracranial Hemorrhage Detection with AI. In *2024, the 7th International Conference on Circuit Power and Computing Technologies (ICCPCT)* (Vol. 1, pp. 138-143). IEEE.

[9] Kaur, S. and Singh, A., 2024. A New Deep Learning Framework for Accurate Intracranial Brain Hemorrhage Detection and Classification Using Real-Time Collected NCCT Images. *Applied Magnetic Resonance*, *55*(6), pp.629-661.

[10] Patel, T.R., Veeturi, S.S., Santo, B.A., Jaikumar, V., Lim, J., Malueg, M.D., Levy, E.I., Siddiqui, A.H., and Tutino, V.M., 2024, November. Deep Learning based Automated Hemorrhage Segmentation and Volume Estimation from Computed Tomography Imaging. In *2024, IEEE Western New York Image and Signal Processing Workshop (WNYISPW)* (pp. 1-5). IEEE.

[11] Yenkikar, A., Mirajkar, R., Sakhare, N., Buchade, A., and Chaudhari, P., Deep Learning in Medical Imaging for Intracranial Hemorrhage Detection and Segmentation. In *Applied Machine Learning in Healthcare* (pp. 313-328). Chapman and Hall/CRC.

[12] Lin, X., Zou, E., Chen, W., Chen, X. and Lin, L., 2025. Advanced multi-label brain hemorrhage segmentation using an attention-based residual U-Net model. *BMC Medical Informatics and Decision Making*, *25*(1), p.286.

[13] Hassan, H.F., Aljobouri, H.K. and Algin, O., 2025. Enhanced Detection of Intracranial Hemorrhage: A New Hybrid Model Design based on the U-Net Segmentation Method. *Iraqi Journal for Computer Science and Mathematics*, *6*(3), p.3.

[14] Rajapakse, J.C., How, C.H., Chan, Y.H., Hao, L.C.P., Padhi, A., Adrakatti, V., Khan, I.R.A., and Lim, T., 2024. Two-stage approach to intracranial hemorrhage segmentation from head CT images. *IEEE Access*, *12*, pp.60839-60848.

[15] Ahmed, S., Esha, J.F., Rahman, M.S., Kaiser, M.S., Hosen, A.S., Ghimire, D., and Park, M.J., 2024. Exploring deep learning and machine learning approaches for brain hemorrhage detection. *IEEE Access*, *12*, pp.45060-45093.

[16] Gençtürk, T.H., Gülağiz, F.K. and Kaya, İ., 2024. Detection and segmentation of subdural hemorrhage on head CT images. *IEEE Access*, *12*, pp.82235-82246.

[17] Chanemougavel, V. and Jayanthi, K., 2025. An End-to-End Multi-Head Attention-Based Deep Learning Model for Enhanced Brain Tumor Detection Using MRI. *Engineering, Technology & Applied Science Research*, *15*(6), pp.30420-30425

[18] Roopitha, C.H., Mayya, V., Sivakumar, V., Patil, V., Pai, D. and Varchas, P., 2026. Enhancing AI-based oral decision support systems: Hybrid image processing for detecting impacted maxillary canines in orthopantomograms. *Intelligence-Based Medicine*, p.100345

[19] Chen, J., Lu, Y., Yu, Q., Luo, X., Adeli, E., Wang, Y., Lu, L., Yuille, A.L. and Zhou, Y., 2021. Transunet: Transformers make strong encoders for medical image segmentation. *arXiv preprint arXiv:2102.04306*

[20] Pratama, I.P.A. and Dewi, N.W.J.K., 2025. Comparative Analysis of Gradient-Based Optimizers in Feedforward Neural Networks for Titanic Survival Prediction. *Indonesian Journal of Data and Science*, *6*(1), pp.90-102

[21] Wang, Y., 2025. Hybrid model integrating LeViT transformer and distillation techniques for pattern detection and dance classification. *Scientific Reports*.

[22] Zhou, J., 2025. A novel hybrid approach for Tornado prediction in the United States: Kalman-convolutional BiLSTM with multi-head attention. *Intelligent Decision Technologies*, *19*(1), pp.194-205

[23] Ameen, M., 2025. Explainable Mammogram Analysis with EfficientNetV2 and Grad-CAM++ for Robust Cancer Diagnosis. *Diagnostics*, *16*(1), p.105.

[24] https://physionet.org/content/ct-ich/1.3.1/

[25] Rajagopal, M., Buradagunta, S., Almeshari, M., Alzamil, Y., Ramalingam, R. and Ravi, V., 2023. An efficient framework to detect intracranial hemorrhage using hybrid deep neural networks. *Brain Sciences*, *13*(3), p.400.

[26] Karamian, A. and Seifi, A., 2025. Diagnostic accuracy of deep learning for intracranial hemorrhage detection in non-contrast brain CT scans: a systematic review and meta-analysis. *Journal of Clinical Medicine*, *14*(7), p.2377.